Drought Responses in Three Apple Cultivars Using an Autonomous Sensor-based Irrigation System

Andrew M. Bierer and Lisa Tang

US Department of Agriculture–Agricultural Research Station, Appalachian Fruit Research Station, 2217 Wiltshire Road, Kearnevsville, WV 25430, USA

Keywords. gas exchange, leaf chlorophyll fluorescence, leaf water potential, Malus ×domestica, water-deficit stress

Abstract. Irrigation decision support systems evolving in the domestic temperate tree fruit production industry incorporate measures of soil moisture status, which diverges from classic physiological indicators of edaphic stress. This study used an autonomous sensor-based irrigation system to impose a water deficit (soil matric potential targets of -25, -40, -60, and -80 kPa) on 'Autumn Gala', 'CrimsonCrisp', and 'Golden Delicious' apple (Malus domestica) cultivars grafted to 'Budagovsky 9' rootstock in the greenhouse (n = 60). It was hypothesized that relationships between physiological plant function, assessed via infrared gas exchange and chlorophyll fluorescence, and the soil matric potential may be used to advance emerging irrigation decision support systems. Complications arising from defoliation by day 11 at -60 and -80 kPa indicate the generation of substrate-specific soil-water relationships in research applications of autonomous sensor-based irrigation systems. 'Autumn Gala' carbon assimilation rates at -80 kPa declined from day 0 to day 8 (9.93 and 5.86 µmol·m⁻²·s⁻¹ carbon dioxide), whereas the transpiration rate was maintained, potentially reducing observed defoliation as other cultivars increased transpiration to maintain carbon assimilation. Correlation matrices revealed Pearson's $r \le |0.43|$ for all physiological metrics considered with soil matric potential. Nevertheless, exploratory regression analysis on predawn leaf water potential, carbon assimilation, transpiration, stomatal conductance, and nonphotochemical quenching exposed speculatively useful data and data shapes that warrant additional study. Nonlinear piecewise regression suggested soil matric potential may useful as a predictor for the rate of change in predawn leaf water potential upon exposure to a water deficit. The critical point bridging the linear spans, -30.6 kPa, could be useful for incorporating in emerging irrigation decision support systems.

Irrigation management choices in commercial temperate fruit production systems vary by region, yet are dominated simply by grower experience or, in fewer cases, by following regional evapotranspiration estimates. Nevertheless, the use of agricultural technology providers and concomitant popularity of decision support platforms is hypothesized to increase as autonomous monitoring technologies mature and the cost barrier to entry declines. Principally, irrigation monitoring technologies can be separated by those using soil-based indicators, weather-based indicators, plant-based indicators, and some combination of the preceding (Osroosh et al. 2016). Currently, numerous decision support platforms

Received for publication 29 Sep 2023. Accepted for publication 9 Jan 2024. Published online 26 Feb 2024.

incorporate soil moisture indicators into irrigation recommendations. Equipment, however, is varied, from applications of remote sensing such as the North American Space Administration's Soil Moisture Active Passive satellite network, unmanned aerial vehicles incorporating agricultural imaging systems (i.e., drones), and ground-based measures consisting of multiple environmental sensor types.

Soil moisture sensors can be divided into those that measure volumetric water content and those that measure the tension (i.e., pressure) of water held in the soil. The volumetric sensor type includes capacitance-based sensors determinant on the capability of the soil to store electric charge, time domain reflectometry sensors measuring the dielectric constant of the soil, and radioactive neutron probes measuring the scattering of neutrons dependent on soil hydrogen content. Tensiontype soil moisture sensors include tensiometers that measure pressure directly and granular matrix sensors that function as a rheostat, a variable resistor dependent on water ingress into the granular matrix. For a more comprehensive discussion of soil moisture sensing, we direct readers to a description by the University of Minnesota Extension (2019). Soil moisture is a commonly used sensing technology for irrigation support systems because

of its lower cost of entry, ease of measurement, and interpretation relative to techniques focusing directly on plant physiology. Some real-time plant physiological monitoring platforms are currently in an early adopter phase, yet the classic measures of plant physiological response to drought stress are point-based handmade measures.

Leaf and stem water potential indicate the internal water status of plants and are used routinely as one of the metrics for quantifying drought responses in woody species including apple (Davies and Lakso 1979; Tworkoski et al. 2016). It has also been established that as leaf water potential declines, stoma closure occurs to prevent water loss via transpiration, thereby limiting atmospheric CO₂ intake and inhibiting photosynthesis (Lakso and Seeley 1978). Therefore, photosynthesis parameters with respect to gas exchange, including photosynthetic carbon assimilation (A), transpiration rate (E), stomatal conductance (g_s), intrinsic water-use efficiency (WUE) (A-to-g_s ratio, indicating a trade-off between photosynthesis and transpiration), and chlorophyll fluoresce, such as quantum yield for photosystem II photochemistry (Sooriyapathirana et al. 2021), are identified as standard indicators for plant physiological changes under a water deficit.

The prior physiological metrics, despite being commonly used in research settings, have a limited commercial adoption as a result of costly equipment requirements, technical proficiencies inconsonant with workforce composition, and 3 lack of autonomy (Rodriguez-Dominguez et al. 2022). These concerns, coupled with the need for continual measurement for the detection of the onset of water deficit stress, have led to commercial movement toward autonomous decision support systems referred to earlier (Jiang and He 2021; Osroosh et al. 2016).

In an academic setting, horticultural drought stress research is typically conducted in one of three ways. First and most commonly, water supply is removed entirely or modified as a percentage of a "typical" event volume (Bhusal et al. 2023). Second, lysimeters can be used to determine precisely the plant water demand using a mass-balance approach for watering, but may be best suited to studies of short duration, which limits the biomass accumulation to avoid entanglement with the inferred water mass balance (Granier et al. 2006; McCauely and Nackley 2022). Third, researchers may derive or measure evapotranspiration dynamics and modify irrigation events conforming to a percentage of total evapotranspiration (Osroosh et al. 2015, 2016). Attempts to study the efficacy of using soil tension sensors for informing irrigation decisions in apple have relied on the "refill" methodology. Herein, two thresholds of soil matric potential are selected for representing wet and dry soil conditions. Irrigation is initiated manually upon sensor readings surpassing the dry threshold and is ceased when the wet threshold is reached, thereby refilling the media's pore space. In prior investigations, both adequate and underirrigation of field-planted apple trees were observed using this methodology compared

Reference of any trade names or commercial products in the article is solely for the purpose of providing specific information and does not imply recommendation or endorsement by the US Department of Agriculture (USDA). The USDA is an equal opportunity provider and employer.

A.M.B. is the corresponding author. E-mail: andrew. bierer@usda.gov.

This is an open access article distributed under the CC BY-NC-ND license (https://creativecommons.org/licenses/by-nc-nd/4.0/).

with competing decision support systems incorporating weather-based and conventional intuition-based approaches (Jiang and He 2021; Osroosh et al. 2016). Additional efforts to maintain soil matric potential in between wet and dry conditions are needed for a more complete understanding of the potential of tension-based soil moisture sensors for irrigation decision support systems. Furthermore, measurement of plant physiological response to drought stress conducted concomitantly with autonomous soil moisture monitoring and control systems can provide practical insights for increasing the utility of soil moisture sensory platforms and decision support systems. One example, in a regression of predawn leaf water potential of potted apple trees by soil water content reported by Tworkoski et al. (2016), suggested the probability of encountering substantially stressful plant water potentials may be deduced from the ratio of the soil water mass to the substrate mass.

Recently, a platform for soil matric potential measurement and sensor-based irrigation automation, Open Irr (USDA-ARS, Kearneysville, WV, USA), was designed for use in horticultural research studies of edaphic stresses (Bierer 2023). The Open_Irr system was designed to use granular matrix Watermark® sensors (Irrometer Co. Inc., Riverside, CA, USA) because they have a lower cost compared with several other soil-based sensor types; as an analog sensor, they are well suited for low-cost data-logging solutions; and tensionbased sensors have a direct tie to plant water availability over volumetric-based sensors. Some disadvantages of the granular matrix Watermark® sensors are that the response time to changes in soil water is on a minutesscale delay; sensor-to-soil contact is critical for proper readings, which leads to a lesser reliability in sandy soils; and soil salinity and temperature can affect readings. Notably, the Open_Irr system allows for long-term horticultural study (i.e., scenarios encountering substantial biomass accumulation or dynamic plant water needs by triggering irrigation events directly and autonomously using Watermark® sensor readings). In this way, the water deficit imposition is fully autonomous and can be studied at various extremities between the typical wet and dry threshold system previously explored for soil tension sensors. Furthermore, research emphasis can be placed on plant physiological response rather than water administration. Therefore, it is of particular interest to examine relationships between the soil matric potential and the scientific standard physiological responses to a water deficit with the ambition of improving emerging decision support systems incorporating soilbased sensing technologies.

This study details the first research trial of the Open_Irr platform for autonomous imposition of drought stress in three apple cultivars—Autumn Gala, CrimsonCrisp, and Golden Delicious—grafted to a common 'Budagovsky 9' rootstock. Despite varying in their fruit quality and disease resistance, these three midseason cultivars are similar in vigor (moderate to moderately high)

and economically important apples in the mid-Atlantic region of study, and thus were selected for this research. The objectives of this study were to identify plant physiological responses to water deficit levels imposed by the Open_Irr system, to determine any influence of scion cultivar grafted on a common rootstock on physiological responses of the trees to a water deficit, and to determine whether useful relationships exist between plant physiological responses and soil moisture status (i.e., the matric potential) that may support emerging decision support systems.

Materials and Methods

Two factors, scion cultivar (Autumn Gala, CrimsonCrisp, and Golden Delicious) and the targeted soil matric potential (-25, -40, -60, and -80 kPa), were considered in a randomized complete block design, with five blocks arranged in north-south rows in a climate-controlled greenhouse. In this arrangement, all cultivar-by-matric potential combinations (n = 12) were present in each block (N = 60). Three pots in each block were assigned the same matric potential target and were considered as a group for the trigger of irrigation events based on the mean soil matric potential. In our study, drought conditions were imposed based on limiting watering events to occur based on a soil matric potential target using the Open_Irr platform (Bierer 2023). Briefly, a municipal water source was routed to distribution manifolds connected to solenoid valves and a 1.9-cm-diameter irrigation dripline with a single emitter installed per pot. Resistive granular matrix type Watermark® sensors were installed in each pot and the sensor readings were used to trigger irrigation events following an algorithm to identify potential outlier sensors and calculate a mean for each three-pot group. The irrigation event duration was 6 s, corresponding to a mean discharge volume of 10.2 mL per event. After an event was triggered, additional events were prohibited for 15 min to allow for a granular matrix sensor response time. For additional information on the irrigation automation setup or the outlier algorithm, a more comprehensive explanation is given in the Open_Irr hardware publication (Bierer 2023).

The potting substrate was specified as a mineral soil to optimize the contact between the Watermark® sensors and substrate because commercial potting media is less effective for resistive-based soil moisture monitoring. Soil was collected from the top 20 cm of a soil profile in Jefferson county, WV, USA, and was classified as a Funkstown silt loam (fineloamy, mixed, active, mesic, Oxyaquic Hapludalfs) based on latitude and longitude by web soil survey (Soil Survey Staff 2021). The soil was collected from a field in perennial hay production with primary constituents of alfalfa (Medicago sativa L.), johnsongrass (Sorghum halepense L.), and orchardgrass (Dactylis glomerata L.). Soil was field-screened to 1 cm then dried at 60 °C before further use. Highdrainage 3150-cm³-square tree pots (with a height of 30.5 cm and a taper of 13 × 13 mm 7.6×7.6 mm) were selected to allow additional height for sensor deployment, enhanced drainage properties, and compatibility with a grid-based support frame constructed in the greenhouse. Cheese cloth was placed over the bottom of each pot to prevent soil passthrough.

Two-year-old bare-rooted nursery trees were potted in the following stages to allow proper deployment of soil moisture and temperature sensors within the rooting zone. First, 725 g of air-dried soil was placed into each pot. Soil moisture and temperature sensors were then held in place as a 2:1 soil-towater mixture was poured to surround and support the Watermark® and calibration-related temperature sensors. The mixture was prepared by mass as 800 g of air-dried soil; the water counterpart was from a municipal source. Pots were left to rest for 5 d to attain partial drying and support the sensors firmly. During this time, 30-cm cotton-fiber wicking cords were installed in each pot by folding one edge of a cord around a flat-head screwdriver and inserting it, through the cheese cloth cover, 5 cm into the bottom of each pot. After 5 d had elapsed, trees were removed from cold storage and pruned to a 10-cm rooting depth and a 70-cm height above the graft union for approximate standardization. On 3 Feb 2022, trees were held in place as 1335 g air-dried soil was poured into the pot around the root tissues. The soil in each pot was pressed gently to ensure stability of the potted trees. Then, 800 mL of municipal water was added to each pot to wet the media thoroughly. The tree diameter 15 cm above the graft union was recorded immediately after planting as the average of north-south and east-west measures using digital calipers. All trees were hand-watered twice per week to saturation while breaking dormancy and accumulating foliage before the period of study. None of the experimental trees produced flowers during the period of study.

On 25 Mar 2022, hand-watering ceased and the water management system of the Open_Irr device was enabled and set to maintain a soil matric potential of all pots at -25 kPa to equilibrate. The Open_Irr device recorded the soil matric potential of each pot on a 15-min interval and opened solenoid valves automatically in between the pressurized municipal water line and dripline leading to respective emitters for 6 s at a time for intended maintenance of the soil matric potential targets. On 16 May 2022, the soil matric potential targets (-25, -40, -60, and -80 kPa) were specified in the Open_Irr device and the water deficit study commenced. The soil matric potential targets were chosen to reflect a generalized soil-water retention curve for the silt loam soil texture (Leong and Rahardjo 1997) and existing literature regarding soil matric potential thresholds for irrigation in apple. Note that substantial desiccation, leading to defoliation, occurred during pot drydown in the -60- and -80-kPa treatments, which restricted the number of measurements made with either fluorometer or infrared gas

analyzer (IRGA) devices on later dates starting 27 May (day 11).

A fluorometer (MultispeQ; PhotosynQ Inc., East Lansing, MI, USA) was used to measure aspects of photosynthetic quenching based on leaf chlorophyll fluorescence on 16, 18, 19, 20, 23, 25, 31 May 2022 and 2, 6, 8, 10, 13 Jun 2022 on two fully expanded leaves per tree. Inadvertently, on 31 May, only a single leaf per tree was measured by the fluorometer. Similarly, a CO₂/H₂O differential (CIRAS-3; PP Systems, Amesbury, MA, USA) was used to measure leaf gas exchange on 17, 18, 20, 23, 25, 31 May and 2, 6, 8, 10, 13 Jun also on two fully expanded leaves per tree. Measurements were acquired at solar noon (~11:30 AM-1:30 PM) to ensure stable environmental conditions (mean air temperature, 29.6 ± 2.9 °C; intensity of photosynthetically active radiation, $471 \pm 338 \, \mu \text{mol} \cdot \text{s}^{-1} \cdot \text{m}^{-2}$). Note that incoming radiation was partially reduced by a conventional greenhouse shading agent (manufacturer unknown) during the period of study. A Scholander pressure chamber (Soil Moisture Equipment Corp., Santa Barbara, CA, USA) was used to observe predawn leaf water potential on 16, 18, 21, 23, 25, 27, 31 May and 2, 6, 8, 10, 13 Jun 2022 on a single leaf from each tree. Leaves were bagged with plastic bags (Whirl-Pak; Filtration Group, Oak Brook, IL, USA) directly before petiole excision at the branch, after which the bag was transferred to the Scholander pressure chamber for pressurization using 99% N2 gas.

Statistical analysis. All analyses were completed using the R programing language (R ver. 4.1.1; Foundation for Statistical Computing, Vienna, Austria) with support of the tidyverse package [tidyverse ver. 1.3.2 (Wickham et al. 2019)] and associated dependencies. Tree diameters were assessed via one-way analysis of variance (ANOVA) by cultivar to determine potential differences in vigor at the beginning of the study. Scholander pressure chamber measurements were

limited by the presence of viable leaves for assessment beginning on 2 Jun 2022. When fluorometer and IRGA measurements were available for two leaves, parameter means were determined and used thereafter. A subset of fluorescence-based parameters: nonphotochemical quenching (NPQt), quantum yield of photosystem II (φ_2), relative fluorescence during or after illumination (Fm'), initial fluorescence during or after illumination (Fo'), maximum quantum efficiency, proton conductivity (gH+), leaf temperature, leaf temperature differential, photosystem I active centers, photosystem I open centers, photosystem I over-reduced centers, photosystem I oxidized centers, and soil plant analysis development relative chlorophyll content (SPAD), and gas exchange parameters— g_s , sub-stomatal CO2 concentration (Ci), leaf temperature, A, E, and WUE-were selected for analysis. It was of interest to identify physiological responses that were correlated with the soil matric potential. Therefore, Pearson's correlation matrices were generated between plant physiological measures and the soil matric potential using the Hmisc [Hmisc ver. 4.8-0 (Harrell Frank and Charles 2021)] and corrplot [corrplot ver. 0.92 (Wei et al. 2021)] packages. To coalesce data sets, soil matric potential data were filtered for observations within time intervals of physiological measurements using the lubridate package [lubridate ver. 1.9.2 (Spinu et al. 2023)]. The mean soil matric potential occurring within the time interval of physiological measurements was determined for each pot and used thereafter. Before generation of the correlation matrix, data were screened for outliers using the Hampel Filter method, in which observations above or below three median absolute deviations were omitted from the Pearson's correlation. All tests were considered significant at a P < 0.05, excluding additional exploratory regression analysis conducted when qualified by Pearson correlation coefficients > |0.2| between the soil matric

potential and photosynthesis-related measures derived from chlorophyll fluorometer and IRGA devices. The photosynthesis-related physiological parameters are summarized in Table 1.

To determine the effects of scion cultivar and water deficit extremity (i.e., treatment), the lme4 and lmerTest packages [lme4 ver. 1.1-31 and lmerTest ver. 3.1-3 (Bates et al. 2015; Kuznetsova et al. 2017)] were used to develop linear mixed-effects models by dependent variable, and days after water deficit imposition using fixed effects of cultivar, the soil matric potential setting, and their interaction, whereas block was considered a random effect. The Satterthwaite method was used for denominator df and all ANOVAs considered significance at P < 0.05. Because the intention was to provide an overview of relationships between plant physiological parameters and the soil matric potential, ANOVA output is presented whereas summary statistics and post-hoc mean separation have been provided as Supplemental Tables 1-5 for additional consideration.

Results

One-way ANOVA indicated, before the start of the study, no significant difference (P=0.275) in scion diameter by cultivar. Scion diameters ranged from 6.7 to 9.6 mm, with a mean of 8.4 mm. At the onset of water deficit imposition, the fully autonomous Open_Irr irrigation system was observed to induce irrigation events corresponding to predetermined soil matric potential thresholds, which continued until study completion (Bierer 2023) (Fig. 1).

Core functionality of the platform to trigger irrigation events was deemed successful; however, mean deviation from the matric potential targets after the first drying curve was common and exacerbated at the -60- and -80-kPa targets as a result of rewetting events and the logarithmic nature of soil water retention. In consequence, results

Table 1. Photosynthesis-related parameters considered in fluorometer and infrared gas analyzer monitoring equipment.

Parameter	Abbreviation	Reference
Leaf chlorophyll fluorescence fluorometer		
Nonphotochemical quenching	NPQ_t	Tietz et al. (2017)
Quantum yield for photosystem II photochemistry	φ_2	Genty et al. (1989)
Relative fluorescence yield during or after illumination	Fm'	Tietz et al. (2017)
Initial fluorescence during or after illumination	Fo'	Tietz et al. (2017)
Maximum quantum efficiency	Fv/Fm'	Kitajima and Butler (1975)
Proton conductivity	gH+	Kanazawa and Kramer (2002)
Leaf temperature	_	PP Systems (2013)
Leaf temperature differential	_	PP Systems (2013)
Fraction of photosystem I active centers	PSI active centers	Kanazawa et al. (2017)
Fraction of photosystem I open centers	PSI open centers	Kanazawa et al. (2017)
Fraction of photosystem I over-reduced centers	PSI over-reduced centers	Kanazawa et al. (2017)
Fraction of photosystem I oxidized centers	PSI oxidized centers	Kanazawa et al. (2017)
Soil plant analysis development relative chlorophyll content	SPAD	Raymond Hunt and Daughtry (2014)
Gas exchange by infrared gas analyzer		
Carbon assimilation	A	PP Systems (2013)
Substomatal CO ₂ concentration	Ci	PP Systems (2013)
Transpiration	E	PP Systems (2013)
Stomatal conductance	$g_{ m s}$	PP Systems (2013)
Leaf temperature	<u> </u>	PP Systems (2013)
Photosynthetic water use efficiency	WUE	PP Systems (2013)

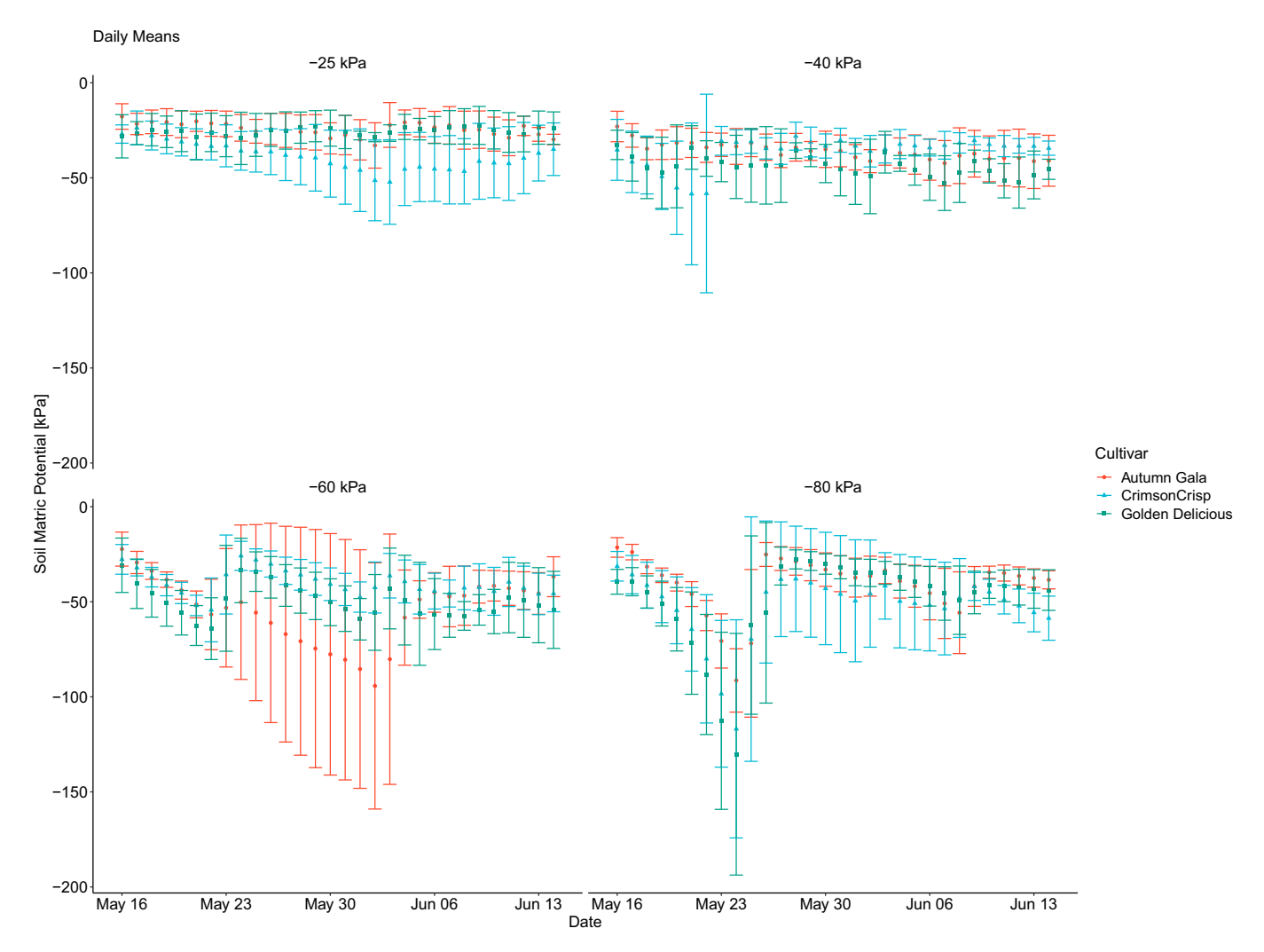


Fig. 1. Daily means and one standard deviation of the mean soil matric potential as observed during the period of study. Four matric potential points (-25, -40, -60, and -80 kPa) were used as irrigation thresholds (i.e., trigger points) for a singular irrigation event in the Open_Irr automation firmware.

presented hereafter may be focused within the context of time-matched observations.

Pearson's correlation matrices between the soil matric potential and plant physiological parameters suggested no significant correlations; nevertheless, correlation coefficients ranged from -0.16 to 0.43 under gas exchange parameters Ci and A, respectively (Figs. 2 and 3). Four gas exchange parameters had correlation coefficients with a soil matric potential > |0.2|, prompting additional exploratory regression analysis.

Å significant intercorrelation among fluorometer or IRGA parameters was more common. Photosystem I measures did not correlate significantly outside of intra-photosystem I comparisons (Fig. 2). Similarly, in 13 of 15 instances, chlorophyll fluorescence measures correlated significantly, although they were not the focus of our study and are not explored here. Relative chlorophyll content correlated significantly with all fluorescence metrics. In the IRGA gas exchange correlation matrix, E and g_s had significant positive correlations with A (r > 0.80) and with each other (r > 0.95) (Fig. 3). Conversely, significant negative correlations were observed between WUE and leaf temperature or Ci

 $(r=-0.5 {\rm \ and } -0.92, {\rm \ respectively})$. Fluorometer-measured leaf temperature held a significant negative correlation with Fm' (P=0.07, r=-0.3), but did not correlate significantly with other fluorescence parameters. Predictably, fluorometer leaf temperature correlated positively with the fluorometer-measured leaf temperature differential (r=0.35).

Additional exploratory regression analysis of IRGA gas exchange parameters WUE, g_s , A, and E produced anticipated patterns of attribute decline with a more negative soil matric potential (Fig. 4).

In the case of WUE, the slope of the linear fit was 0.02, whereas $r^2 = 0.12$. Each other IRGA gas exchange parameter $(g_s, A, \text{ and } E)$ followed a quadratic relationship with the soil matric potential; coefficients of determination were 0.12, 0.15, and 0.20, respectively, for g_s , A, and E. Anecdotally, critical inflection points could be discerned visually in the g_s and E regressions; however, least-squares model selection did not attribute any statistical advantage to a more complex two-linear fit.

Conversely, predawn leaf water potential was plotted against the soil matric potential, following preceding work by Tworkoski et al. (2016). In our study, this regression followed a two-linear fit. The critical point was identified as -30.6 kPa, which corresponded to a plant water potential of -0.73 MPa ($r^2 = 0.29$) (Fig. 5).

Analysis of variance indicated a significant effect of treatment on predawn leaf water potential beginning 2 d after water deficit imposition, which largely persisted throughout the study (Table 2). There was not substantial evidence to suggest a significant effect of cultivar on predawn leaf water potential outside of irregular occurrence on days 23 and 25 of deficit imposition. We suggest these two observations originated from a shortage of suitable leaves for measurement as a result of defoliation during later stages of deficit imposition.

Analysis of variance suggested IRGA gas exchange parameters were far more sensitive to scion cultivar relative to predawn leaf water potential. Analysis of variance suggested A, E, g_s , and leaf temperature had significant cultivar-by-treatment interactions on multiple days after deficit imposition (Table 3). This article intends to identify responsive plant

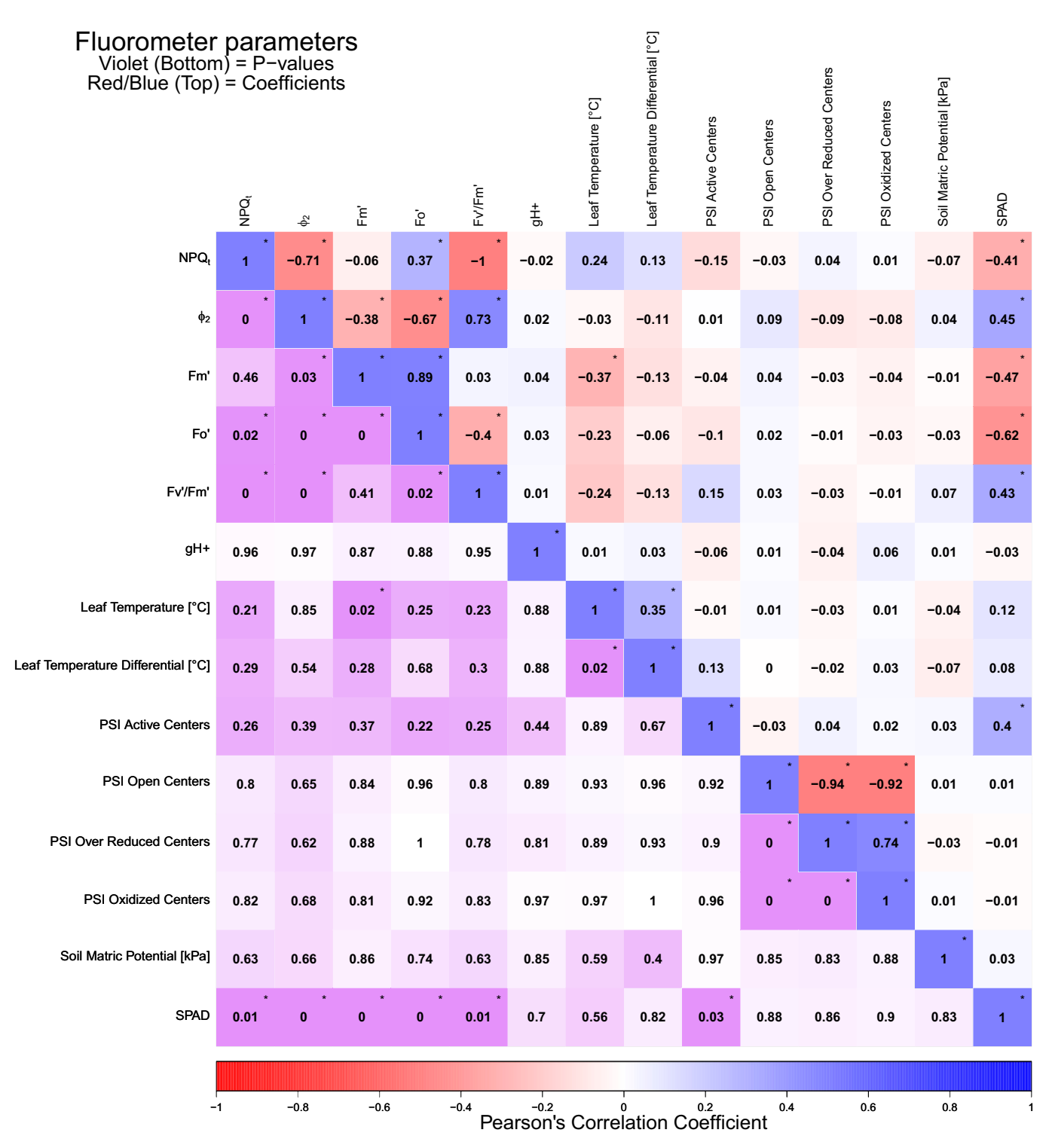


Fig. 2. Pearson's correlation coefficient matrix containing leaf chlorophyll fluorescence parameters and the soil matric potential. The top portion of the matrix contains correlation coefficients whereas the bottom portion of the matrix contains correlation P values. Cells of the matrix identified with an asterisk in the top right corner of the cell were considered significant at P < 0.05. Additional regression analysis between the soil matric potential and physiological parameters was conducted on correlation coefficients > |0.2|. Fm' = relative fluorescence yield during or after illumination; Fo' = initial fluorescence during or after illumination; Fv'/Fm' = maximum quantum efficiency; gH+ = proton conductivity; NPQt = nonphotochemical quenching; PS = photosystem; σ_2 = quantum yield for photosystem II photochemistry; SPAD = soil plant analysis development chlorophyll content.

physiological parameters to water deficit that have potentially useful relationships with the soil matric potential. Further exploration of cultivar differences on specific parameters was beyond the scope of our study; however, we remind readers that summary statistics and post hoc testing has been provided for consideration as Supplemental Tables 1–5 for predawn leaf water potential, A, E, WUE, and $g_{\rm s}$.

In contrast, Ci and WUE were unaffected by scion cultivar outside of days 14 and 16 of deficit, when the WUE of 'Autumn Gala' declined, respectively, by a factor of 0.52 and $0.64~\mathrm{under}$ $-80~\mathrm{kPa}$ relative to 'CrimsonCrisp' and 'Golden Delicious' cultivars.

'CrimsonCrisp' observed an increase in A of 4.9 μ mol $CO_2 \cdot m^{-2} \cdot s^{-1}$ over 'Autumn Gala' and 'Golden Delicious' cultivars at –80 kPa when pooling days after deficit imposition. 'Autumn Gala' was observed to be

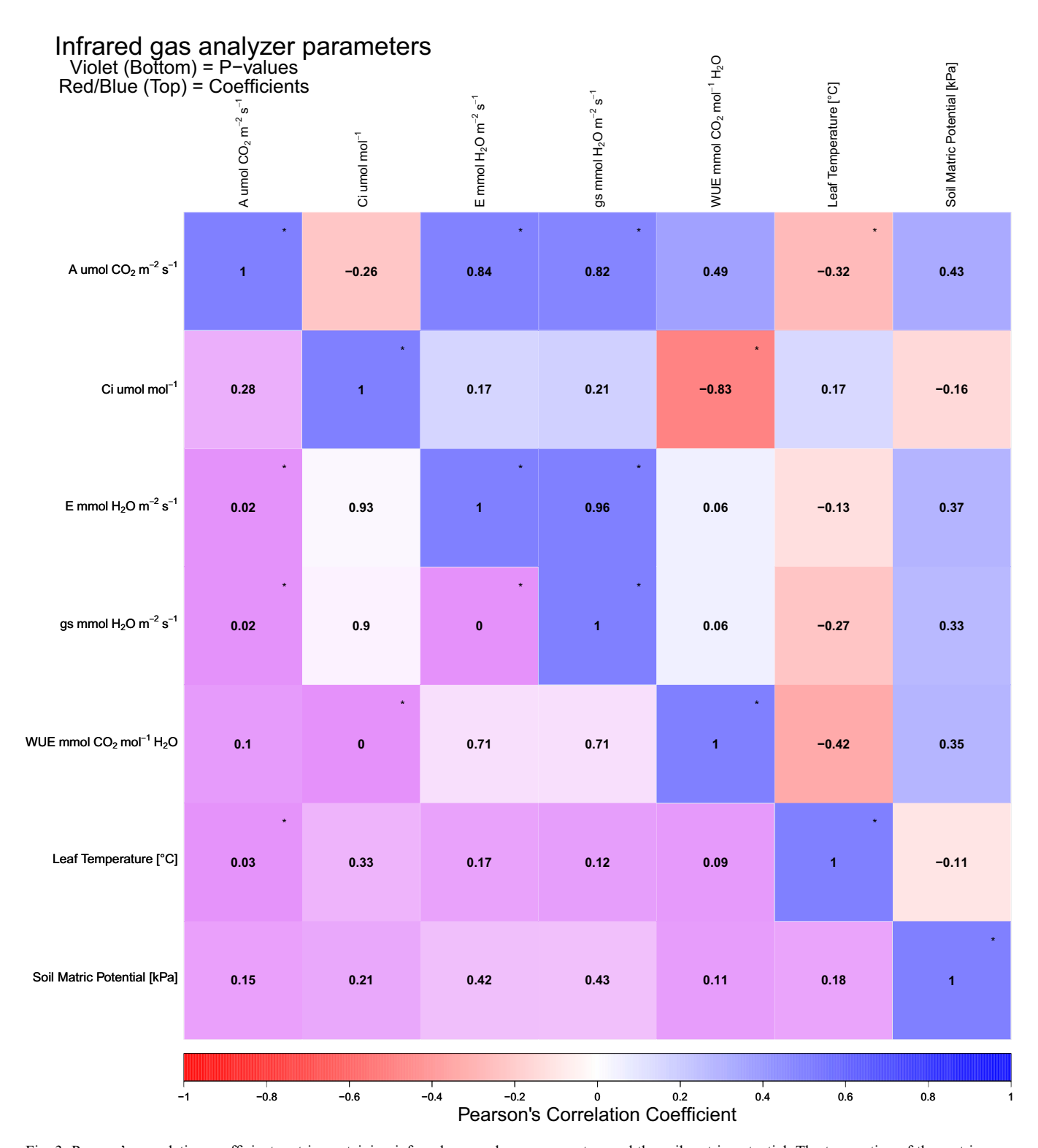


Fig. 3. Pearson's correlation coefficient matrix containing infrared gas exchange parameters and the soil matric potential. The top portion of the matrix contains correlation coefficients whereas the bottom portion of the matrix contains correlation P values. Cells of the matrix identified with an asterisk in the top right corner of the cell were considered significant at P < 0.05. Additional regression analysis between the soil matric potential and physiological parameters was conducted on correlation coefficients > |0.2|. A = photosynthetic carbon assimilation; Ci = substomatal CO₂ concentration; E = transpiration rate; g_s = stomatal conductance; WUE = water-use efficiency.

the least-efficient assimilator under the driest conditions at -80 kPa, yet outperformed 'CrimsonCrisp' and 'Golden Delicious' at -60 and -40 kPa. Transpiration rates at -80 kPa followed suit; 'Autumn Gala' E was less than that of 'CrimsonCrisp' and 'Golden Delicious' by a factor of 0.59. Predictably,

pooled g_s at -80 kPa was less for 'Autumn Gala' (53.9 mmol $CO_2 \cdot mol^{-1}$ H_2O) than 'CrimsonCrisp' (122.5 mmol $CO_2 \cdot mol^{-1}$ H_2O) or 'Golden Delicious' (95.3 mmol $CO_2 \cdot mol^{-1}$ H_2O). A significant cultivar-by-treatment interaction was indicated on 8 of 10 d for IRGA-measured leaf temperature observations. On a

macroscale, leaf temperature shadowed weekly temperature patterns as minor incremental changes occurred within the greenhouse. The first to third quartile range of observed temperature was 32.7 to 34.9 °C during the period of deficit imposition. Infrared gas analyzer—measured leaf temperature was 0.65 °C less on

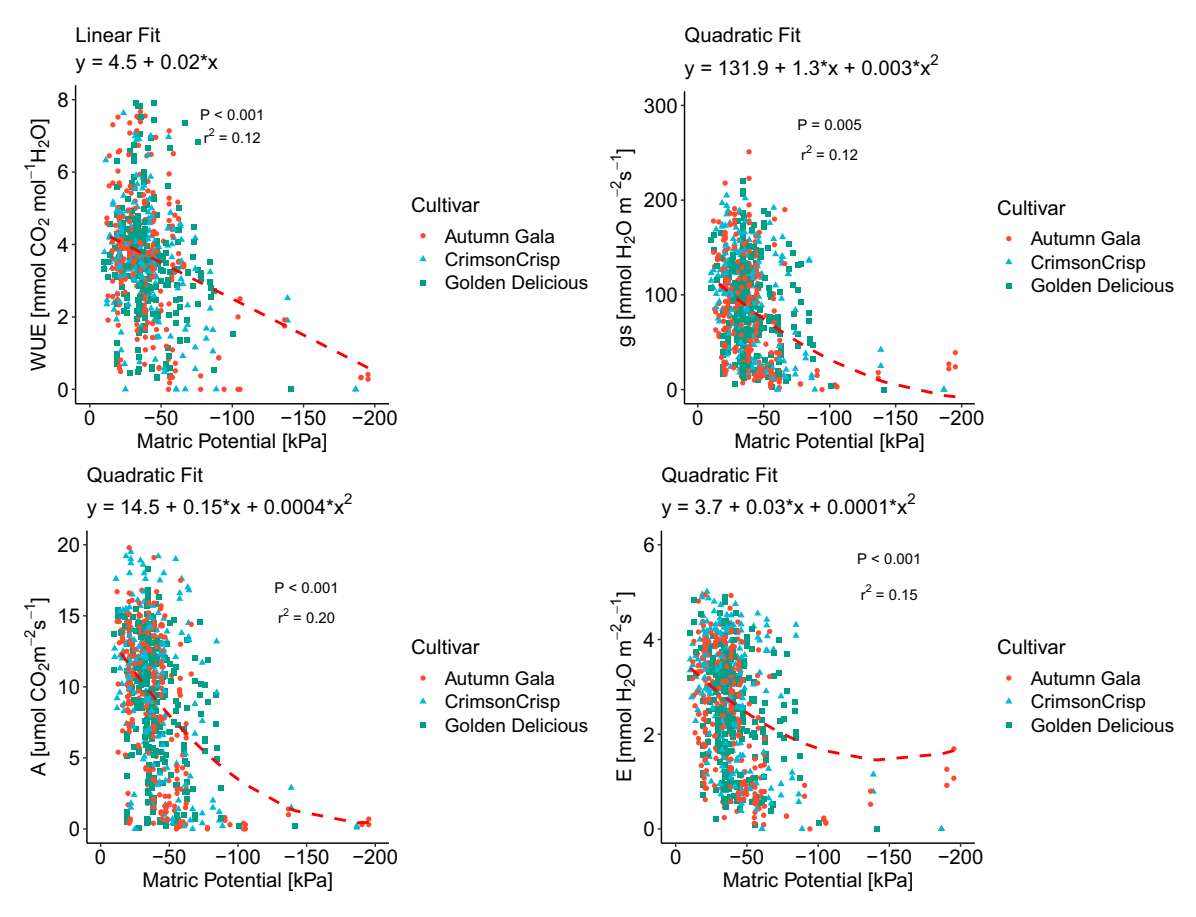


Fig. 4. Exploratory regression analysis of selected infrared gas exchange parameter observations against the soil matric potential. Water use efficiency (top left); stomatal conductance (top right); carbon assimilation (bottom left); transpiration (bottom right). Model selection was performed using the method of nonlinear least squares and appropriate fit statistics. Converging models containing fewer terms were selected when similar fit statistics were observed.

average for 'CrimsonCrisp' trees relative to 'Autumn Gala' and 'Golden Delicious' cultivars during the period of deficit imposition. A significant interaction effect for IRGA-measured leaf temperature on individual days likely originates from the variance in cultivar E rates.

Analysis of variance conducted on chlorophyll fluorescence parameter measures generally suggest the effects of cultivar and/or treatment were intermittent (Table 4).

On day 0, mean NPQ_t of 'CrimsonCrisp' (0.262) was significantly less than that of

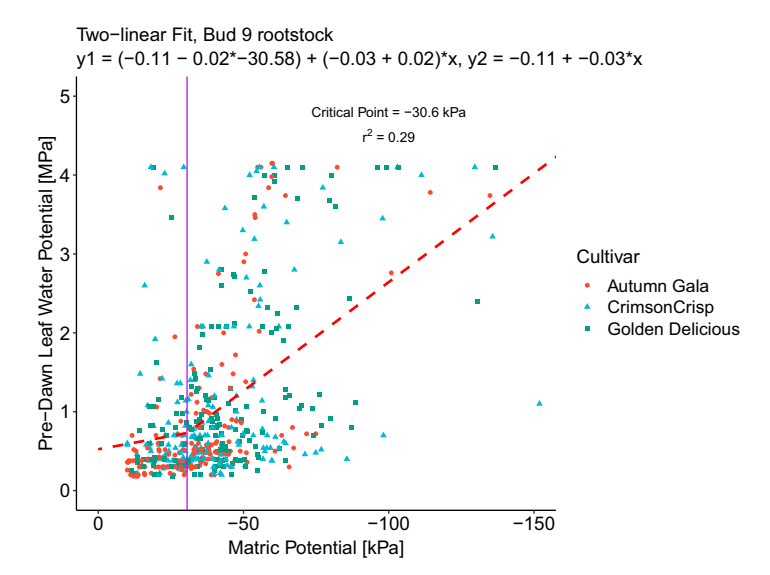


Fig. 5. Predawn leaf water potential as influenced by the soil matric potential during the period of study. The two-linear fit was obtained using nonlinear least squares. The breakpoint (-30.6 kPa) was determined by allowing the slope of the left line to be a function of the critical point and other model parameters.

'Autumn Gala' (0.462). When pooling all observations, 'Autumn Gala' held a +19% differential in NPQt over 'CrimsonCrisp' and 'Golden Delicious'. Only by day 7 was NPQt observed to increase clearly, according to deficit extremity, spanning from 0.583 at -25 kPa to 1.56 at -80 kPa. From days 8 to 10, watering events triggered in the -60- and -80-kPa treatments rewetted planting containers, which presumably led to declines in NPQ_t on day 15 relative to day 7 (Fig. 1). From 21 to 28 d after deficit imposition, NPO_t resumed the trend of increasing with edaphic drought stress level. Nevertheless, this did not manifest in the Pearson's correlation matrix (Fig. 2).

Day 0 φ_2 measurements suggested minor differences between 'Autumn Gala' (0.594) 'CrimsonCrisp' (0.626), and 'Golden Delicious' (0.599), which did not persist for the remainder of the study (Table 4). On day 7, a significant effect of treatment was suggested, as the mean φ_2 value at -25 kPa (0.505) was greater than the φ_2 value at -80 kPa (0.410). Albeit at a lesser differential, similar differences produced the significant treatment effect noted on days 9 and 21 (Table 4).

Relative fluorescence yield was largely unresponsive to cultivar and water deficit extremity. On day 7, a significant treatment effect was observed, as mean Fm' value at -25 kPa (4544) was significantly greater than

Table 2. Type III analysis of variance P values (significant at P < 0.05) of predawn leaf water potential as affected by scion cultivar, soil matric potential setting (i.e., treatment), and their interaction.

	Days elapsed											
Variable	0	2	5	7	9	11	15	17	21	23	25	28
Scion	0.342	0.454	0.530	0.303	0.376	0.659	0.754	0.410	0.652	< 0.001	0.074	0.381
Treatment	0.996	0.005	< 0.001	< 0.001	< 0.001	0.117	< 0.001	0.062	< 0.001	< 0.001	< 0.001	0.002
Scion × Treatment	0.787	0.998	0.413	0.714	0.146	0.618	0.716	0.855	0.874	0.001	0.329	0.915

Fm' at -80 kPa (3270). Similarly, on day 23, the mean Fm' value at -25 kPa (5099) was significantly different from the mean Fm' value at -60 kPa (4497).

For the related parameter Fo', there was no evidence of a significant cultivar-by-treatment interaction. On days 2, 3, 17, and 23, a significant effect of cultivar was suggested; Fo' tended to be greatest for 'Autumn Gala'. Pooling all days, mean Fo' was, respectively, 1066, 998, and 1002 for 'Autumn Gala', 'Crimson Crisp', and 'Golden Delicious'. A significant treatment effect on Fo' was indicated on days 17 and 23. Model-estimated marginal means suggested Fo' was significantly greater at -60 kPa relative to all other treatments.

There was no evidence of an effect of cultivar on gH+, despite a cultivar-by-treatment interaction suggested on days 2 and 3, when gH+ of 'CrimsonCrisp' was greater than either 'Autumn Gala' or 'CrimsonCrisp' at -25 kPa. Proton conductivity was responsive to treatment on days 2 through 7, 21, and 25; after pooling all days, mean gH+ at -25 kPa (157) was numerically greater than at -40 kPa (142) and -60 or -80 kPa (both equal to 128).

Unlike the IRGA apparatus, leaf temperature recorded by the fluorometer did not suggest differences by cultivar; however, a significant effect of water deficit (i.e., treatment) was still suggested on days 2 through 9, 23,

and 25. Temperature means in the –25-, –40-, –60-, and –80-kPa treatments pooled across all days were, respectively, 25.6, 25.9, 26.3, and 26.6 °C. The largest numerical difference between treatments occurred on day 7, when the mean leaf temperature at –25 kPa (23.4 °C) was considerably less than that at –80 kPa (25.6 °C). The leaf temperature differential was less responsive to either cultivar or treatment. The presence of a significant effect of treatment was indicated only on day 4 of deficit imposition, when the delta from ambient values for the –25-, –40-, –60-, and –80-kPa treatments were –4.0, –3.7, –2.3, and –1.9 °C, respectively.

Chlorophyl fluorescence parameters describing aspects of reaction centers within photosystem I complexes were not equivalently responsive to effects of cultivar or treatment. Photosystem I active centers were most responsive whereas open centers, overreduced centers, and oxidized centers suggested a less frequent occurrence of any effect, despite happening concurrently on days 3, 4, 17, and 21. The photosystem I active center parameter responded to both cultivar and treatment. Pooling scion cultivars at -25 kPa resulted in a positive linear relationship of photosystem I active center measures with time, with a slope of 0.025. Conversely, at -40 kPa, photosystem I active centers were stable, but declined across time at -60 and

-80 kPa. Pooling days in the -25-kPa treatment, mean photosystem I active centers were, respectively, 2.55, 3.45, and 2.80 for 'Autumn Gala', 'CrimsonCrisp', and 'Golden Delicious'. This variance by cultivar did not persist at -60 or -80 kPa. At -60 kPa, the pooled mean photosystem I active centers were 2.63, 2.42, and 2.82 for 'Autumn Gala', 'CrimsonCrisp', and 'Golden Delicious', respectively.

Relative chlorophyll content was able to differentiate between scion cultivars on 7 of 12 d of measure, including day 0 before imposition of water deficit. Mean SPAD of 'Autumn Gala', 'CrimsonCrisp', and 'Golden Delicious' cultivars on day 0 was, respectively, 53.7, 61.2, and 57.3, which declined to 46.4, 52.6, and 49.8 by day 7 of water deficit imposition (i.e., the primary drying curve). A significant treatment effect was indicated on days 2, 17, 21, 25, and 28; however, the Pearson's correlation matrix did not identify separately a practical relationship between SPAD and the soil matric potential (Fig. 2).

Upon exhumation of rooting systems, ANOVA suggested no difference in rooting depth among scion cultivar or soil matric potential targets, as 40 of 60 trees had rooted to the maximum depth permitted by the pots (30.0 cm), whereas the remainder had rooted to depths $\geq 28.0 \text{ cm}$. Consider, though, that

Table 3. Type III analysis of variance P values (significant at P < 0.05) of infrared gas analyzer gas exchange parameters as affected by scion cultivar, soil matric potential setting (i.e., treatment), and their interaction.

Parameter	Days elapsed												
	0	1	3	6	8	14	16	20	22	24	27		
Carbon assimilation													
Scion	0.076	0.001	0.001	0.016	0.293	0.011	< 0.001	< 0.001	_	0.006	0.084		
Treatment	0.678	0.296	< 0.001	0.144	0.070	0.244	0.302	0.190	_	0.157	0.269		
Scion × Treatment	0.184	0.007	< 0.001	0.012	0.001	< 0.001	< 0.001	< 0.001	_	0.003	0.309		
Transpiration													
Scion	0.380	0.002	< 0.001	< 0.001	0.291	< 0.001	< 0.001	0.003	_	0.013	0.069		
Treatment	0.517	0.022	< 0.001	0.038	0.085	0.016	0.349	0.122	_	0.398	0.184		
Scion × Treatment	0.037	0.009	< 0.001	0.004	< 0.001	< 0.001	< 0.001	0.003	_	0.049	0.270		
Substomatal CO ₂ concer	ntration												
Scion	0.099	0.424	0.743	0.869	0.898	0.677	0.601	0.911	_	0.419	0.480		
Treatment	0.356	0.012	0.397	0.832	0.012	0.347	0.752	0.444	_	0.008	0.741		
Scion × Treatment	0.246	0.293	0.508	0.124	0.297	0.007	< 0.001	0.900	_	0.839	0.718		
Stomatal conductance													
Scion	0.758	0.002	< 0.001	< 0.001	0.188	< 0.001	< 0.001	0.001	_	0.013	0.031		
Treatment	0.517	0.040	< 0.001	0.066	0.059	0.014	0.139	0.070	_	0.384	0.254		
Scion × Treatment	0.039	0.018	< 0.001	0.002	< 0.001	< 0.001	< 0.001	0.003	_	0.057	0.210		
Leaf temperature													
Scion	0.055	0.424	< 0.001	0.635	0.002	< 0.001	0.226	0.043	_	0.011	0.010		
Treatment	0.332	0.346	0.110	0.134	0.125	0.435	0.467	0.715	_	0.698	0.096		
Scion × Treatment	0.009	0.747	0.001	0.002	0.035	< 0.001	0.001	< 0.001	_	0.002	0.231		
Water use efficiency													
Scion	0.105	0.510	0.240	0.359	0.898	0.283	0.134	0.216	_	0.352	0.164		
Treatment	0.523	0.029	0.481	0.389	0.006	0.503	0.819	0.650	_	0.118	0.318		
Scion × Treatment	0.083	0.057	0.155	0.176	0.135	< 0.001	< 0.001	0.083	_	0.885	0.649		

¹ Twenty-two days after deficit imposition a lack of viable readings prevented model convergence.

Table 4. Type III analysis of variance P values (significant at P < 0.05) of photosynthesis-related measurements based on leaf chlorophyll fluorescence as affected by scion cultivar, soil matric potential setting (i.e., treatment), and their interaction.

Variable	Days elapsed												
	0	2	3	4	7	9	15	17	21	23	25	28	
Nonphotochemical quenc	hing												
Scion	0.001	0.070	0.626	0.363	0.650	0.114	0.481	0.147	0.031	0.008	0.007	0.057	
Treatment	0.516	0.592	0.018	0.003	< 0.001	< 0.001	0.700	0.346	< 0.001	< 0.001	< 0.001	0.072	
Scion × Treatment	0.664	0.384	0.706	0.988	0.243	0.181	0.508	0.839	0.091	0.186	0.596	0.046	
Quantum yield													
Scion	0.037	0.821	0.273	0.806	0.962	0.514	0.545	0.181	0.549	0.583	0.391	0.166	
Treatment	0.570	0.767	0.973	0.815	0.012	0.023	0.930	0.206	0.015	0.093	0.500	0.305	
Scion × Treatment	0.847	0.638	0.772	0.996	0.772	0.635	0.424	0.984	0.900	0.921	0.953	0.663	
Relative fluorescence yiel	ld												
Scion	0.943	0.227	0.116	0.971	0.586	0.982	0.654	0.770	0.363	0.245	0.385	0.519	
Treatment	0.713	0.387	0.062	0.157	0.016	0.519	0.547	0.734	0.536	0.037	0.102	0.253	
Scion × Treatment	0.614	0.038	0.670	0.988	0.898	0.957	0.901	0.871	0.695	0.497	0.716	0.602	
Initial fluorescence													
Scion	0.232	< 0.001	< 0.001	0.787	0.270	0.847	0.421	0.001	0.737	0.022	0.092	0.785	
Treatment	0.600	0.156	0.270	0.924	0.801	0.602	0.228	< 0.001	0.773	0.012	0.775	0.147	
Scion × Treatment	0.661	0.033	0.902	0.996	0.826	0.822	0.787	0.102	0.960	0.113	0.865	0.572	
Maximum quantum effici	ency												
Scion	< 0.001	0.078	0.657	0.325	0.719	0.102	0.515	0.124	0.048	0.004	0.005	0.050	
Treatment	0.492	0.555	0.015	< 0.001	< 0.001	< 0.001	0.661	0.292	< 0.001	< 0.001	< 0.001	0.077	
Scion × Treatment	0.684	0.349	0.697	0.989	0.219	0.203	0.526	0.838	0.102	0.198	0.675	0.056	
Proton conductivity													
Scion	0.470	0.663	0.395	0.770	0.627	0.609	0.447	0.356	0.170	0.871	0.220	0.232	
Treatment	0.633	0.032	0.032	0.015	0.007	0.567	0.053	0.176	0.004	0.209	0.040	0.121	
Scion × Treatment	0.606	0.015	0.024	0.766	0.689	0.668	0.961	0.084	0.731	0.212	0.868	0.774	
Leaf temperature													
Scion	0.443	0.044	0.213	0.785	0.326	0.727	0.540	0.383	0.444	0.467	0.160	0.605	
Treatment	0.652	0.002	0.003	< 0.001	< 0.001	0.004	0.192	0.730	0.094	0.018	< 0.001	0.933	
Scion × Treatment	0.435	0.858	0.667	0.736	0.795	0.646	0.679	0.905	0.682	0.243	0.185	0.038	
Leaf temperature differen	tial												
Scion	0.518	0.545	0.644	0.941	0.761	0.503	0.312	0.085	0.783	0.890	0.455	0.814	
Treatment	0.746	0.157	0.024	< 0.001	0.328	0.799	0.445	0.771	0.359	0.175	0.010	0.165	
Scion × Treatment	0.963	0.929	0.989	0.852	0.954	0.624	0.527	0.816	0.974	0.413	0.802	0.980	
Photosystem I active cent	ters												
Scion	0.004	0.553	0.001	0.075	0.050	0.081	0.313	0.095	0.240	0.066	0.328	0.067	
Treatment	0.013	0.056	0.017	0.105	0.009	0.003	0.467	0.003	< 0.001	0.178	< 0.001	0.050	
Scion × Treatment	0.742	0.283	0.605	0.959	0.015	0.031	0.519	0.168	0.001	0.401	0.026	0.180	
Photosystem I open cente	ers												
Scion	0.372	0.714	0.074	0.023	0.930	0.722	0.719	0.746	0.009	0.965	0.726	0.654	
Treatment	0.297	0.632	0.112	0.032	0.369	0.824	0.491	0.763	0.012	0.455	0.610	0.661	
Scion × Treatment	0.422	0.791	0.086	0.346	0.846	0.274	0.714	0.387	0.248	0.363	0.734	0.788	
Photosystem I over-reduc	ed centers												
Scion	0.746	0.765	0.031	0.212	0.837	0.752	0.790	0.009	0.414	0.803	0.785	0.525	
Treatment	0.163	0.683	0.035	0.320	0.241	0.826	0.386	0.071	0.015	0.401	0.659	0.773	
Scion × Treatment	0.795	0.675	0.525	0.289	0.081	0.353	0.930	0.061	0.170	0.301	0.694	0.523	
Photosystem I oxidized c	enters												
Scion	0.504	0.770	0.118	0.289	0.762	0.839	0.597	0.048	0.030	0.190	0.609	0.439	
Treatment	0.163	0.706	0.079	0.484	0.328	0.917	0.607	0.243	0.118	0.527	0.532	0.880	
Scion × Treatment	0.715	0.616	0.114	0.248	0.036	0.631	0.582	0.194	0.271	0.508	0.752	0.329	
Soil plant analysis develo	pment relati	ve chloroph	yll content										
Scion	< 0.001	< 0.001	< 0.001	0.012	0.032	0.244	0.165	0.009	0.038	0.131	0.362	0.865	
Treatment	0.274	0.015	0.161	0.196	0.096	0.354	0.537	0.032	< 0.001	0.125	0.005	0.003	
Scion × Treatment	0.110	0.044	0.519	0.869	0.231	0.483	0.502	0.353	0.075	0.110	0.742	0.631	

rooting systems developed before the onset of the study after planting occurred on 3 Feb 2022, and the available pot volume was limited to 3150 cm³.

Discussion

Irrigation events were occurring regularly at the -25- and -40-kPa thresholds 2 d after the onset of the trial; however, events were not triggered until 23 and 24 May at -60 and -80 kPa, respectively (Fig. 1). Substantive desiccation of tree foliage had occurred by this time in the -60- and -80-kPa treatments, suggesting that the related reduction in plant water requirements thereafter, at least in part, contributed to the soil matric potential dynamics

observed. In effect, the wet-dry-like cyclic nature of the soil matric potential encountered during these treatments is expected to be a function of the irrigation parameters in Open_Irr, along with the plant water demands during drying and the recovery wetting curves. Elsewhere, -80 kPa has been used as a threshold for irrigation events to refill the soil profile in field-planted apple (Bhusal et al. 2019; Jiang and He 2021; Osroosh et al. 2016), with reporting varying from minor or moderate underirrigation to satisfactory. These preceding studies were implemented in fieldgrown apple trees where access to greater soil depth, and therefore volume, in addition to unlimited rooting systems may be less detrimental to tree health. Our study supplements existing literature specifically by examining potted apple trees

using a soil matric potential-driven irrigation practice.

Pearson's correlation matrix of fluorometer measures failed to identify relationships between physiological photosynthesis measures and the soil matric potential (Fig. 2). As subsequent ANOVAs suggested, select parameters (NPQ_t, φ₂, Fo', gH+) responded to deficit treatments primarily during the first and last week of the study. It may be that drying cycle dynamics, at least in part, obfuscated the nature of this relationship. For example, Fo' was greater on average in the −60-kPa treatment on days 17 and 21 relative to all other treatments. Likewise, the soil water content was numerically greater in the −60-kPa treatment relative to the −80-kPa

treatment, which manifested from a combination of a lag period between the Open_Irr system triggering brief, 6-s irrigation events and substantive refill of the container pore space to reach the soil matric potential sensors; and a sharp decline in plant water demand in the -80-kPa treatment after desiccation and defoliation (Fig. 1). This pattern also presented itself with gH+ (Fig. 2); elsewhere, gH+ in wheat (*Triticum aestivum*) was unresponsive only during moderate drought conditions (Zivcak et al. 2014).

Differences in chlorophyll florescencebased NPQ_t and φ₂ of scion cultivars on day 0 indicate the inherent (genetic) differences related to the photosynthetic apparatus, which may contribute to varied stomatal control among the cultivars and therefore differences in gas exchange readings, including A, E, g_s , during the first week of water deficit imposition. Nevertheless, plant water status, as indicated by the leaf water potential of scion cultivars, was not significantly different on any data collection day at any soil moisture level. It is of interest that the leaf water potential of 'Autumn Gala' was numerically greater (less negative) than that of 'Crimson-Crisp' and 'Golden Delicious' on day 2 of the -60- and -80-kPa treatments, respectively, with no readings less than -1.5 MPa. During both treatment conditions, the leaf water potential of all varieties decreased drastically to severe levels (<-3.0 MPa) on day 5. It is therefore possible that the difference by cultivar in plant water status took place between the two sampling days and may not have been captured by our study.

Gas exchange rate measures A and E suggest different survival strategies among the cultivars studied. Carbon assimilation of 'Autumn Gala' in the -80-kPa treatment was observed to decline from day 0 (9.93 µmol $CO_2 \cdot m^{-2} \cdot s^{-1}$) to day 8 (5.86 µmol $CO_2 \cdot m^{-2} \cdot s^{-1}$), whereas both 'CrimsonCrisp' and 'Golden Delicious' maintained A while increasing E by an average of 47% over the same period. This downregulation of photochemistry is known to be an important defense mechanism against the onset of water deficit conditions (Chaves et al. 2002). A similar observation to our study was made previously in a comparison of 'Fuji' and 'Gala' apples. Upon withholding water completely for 4 d, it was reported that 'Gala' decreased A rates by nearly 90%, whereas during the same period 'Fuji' declined by only 47% (Tworkoski et al. 2016). Thus, it appears that 'Gala' has a greater proclivity for stomatal regulation as a defense mechanism against water deficit. Likewise, perhaps 'CrimsonCrisp' and 'Golden Delicious' exhibit nonstomatal factors that contribute to decreased A under water stress, as explained by Wang et al. (2018).

The most extreme drought treatment of this study (the soil matric potential at –80 kPa) resulted in leaf water potential values less than –1.5 MPa, the threshold value for reportedly significant drought stress in apple (Tworkoski et al. 2016), within 7 d for the three apple cultivars tested. Trees in this treatment also experienced desiccation progressing to defoliation during the primary drying curve after the onset of the trial (Fig. 1). Measurement of the leaf

water potential therefore became limited, progressing to impossible, in some replicates staring at day 11 for 'CrimsonCrisp' and 'Golden Delicious', and at day 15 for 'Autumn Gala', even though photosynthesis-related data were still recorded with the remaining leaves throughout the experiment in all trees. Notably, irrigation events prompted by the Open_Irr system in response to a soil water deficit subsequently promoted the growth of new flushes in defoliating trees (Fig. 1). Thus, the physiological data collected in trees at -80 kPa on later days may either still demonstrate drought-triggered responses (as in 'Autumn Gala', which had relatively moderate leaf abscission) or may reflect a postdrought recovery process (as in 'CrimsonCrisp', with new foliage after all five individual-tree replicates lost viable leaves for water potential quantification on day 17). This possibility could support, in part, the greater g_s and A in actively growing leaves of 'CrimsonCrisp' than that of stress-induced senescing leaves of 'Autumn Gala' at -80 kPa when pooling days after deficit imposition. The inference is consistent with the increase in both g_s and A from the drought stress period to rehydration (recovery) in potted 'Gamhong' apple on 'M.9' rootstock (Bhusal et al. 2023).

Our results demonstrate that the soil matric potential, when < -30.6 kPa, explained 29% of the variation in the leaf water potential in apple trees. This critical point of soil water content corresponded to the leaf water potential of -0.73 MPa, within the range of water status for nonstressed plants [i.e., < -1.5 MPa for apple (Tworkoski et al. 2016)], suggesting the applicability of this model in predicting plant water status, to a certain extent, before significant water deficit stress. The critical point corresponding to a leaf water potential of -0.73 MPa as a potentially useful management threshold is comparable to a similar report of -0.55 MPa in mandarin (Citrus reticulata) trees (Maotani and Machida 1980). It is interesting, though, that the threshold indicated by our study pertains to the soil matric potential and is within the range of field capacities (-10 to -33 kPa) for various soil textures. One possible explanation is the transition from plant use of gravimetric to capillary water stores for maintenance of turgor. Regardless of rationale, we hesitate to recommend the -30.6-kPa soil matric potential threshold for use as a singular indicator for irrigation needs because, conceptually, this corresponds with a known adequate water supply for the majority of soils.

Several "extreme" observations of predawn leaf water potential occurred concomitantly with a soil matric potential ≥ -25 kPa. We suggest this is an artifact of the timing and nature of the automated watering system and/or a recovery period after an irrigation event. Irrigation water could have followed preferential flow paths in the drying soil (e.g., voids surrounding sensor wires or roots), rapidly reaching the Watermark sensors before sufficient rewetting of the surrounding soil matrix. In addition, a day-scale delay between the cessation of drought stress and

hydraulic recovery has been reported in field-planted 'Gamhong' apple (Bhusal et al. 2023), which could also explain the several counterintuitive observation points. Conversely, potted apple trees have been reported to respond rapidly to rewetting with attempts to maintain the water potential at target levels (Tang and Lovatt 2022). Regardless, we recommend future endeavors using automated watering equipment to implement stresses more gradually at the onset of study and to fine-tune irrigation events to avoid obfuscating responses upon water additions, because they are not as useful for developing management thresholds. For instance, predawn leaf water potential and photosynthesis readings obtained after day 15 in the -60-kPa and -80-kPa treatments used primarily newly produced leaves following rewetting after respective thresholds were crossed. To this end, future experimental design should focus on mild to moderate drought treatments by considering soil substrate and media-specific water relations, which, in a commercial setting, may also be more common than extreme or abrupt drought, as fruit growers typically strive to avoid detrimental effects on yield or quality, as when practicing deficit irrigation for size or bitter pit control (Reid and Kalcsits 2020). Anecdotally, it was confirmed that derivation of a soil-specific soil water retention curve improved implementation of edaphic stress during subsequent investigations during Summer 2023 (Bierer, unpublished data). Therefore, we emphasize the utility of generating a water retention curve before the use of the Open_Irr system, especially for academic purposes.

The exploratory regression analysis conducted on IRGA gas exchange parameters (A, E, g_s, and WUE) produced a generally poor fit with the soil matric potential (all r^2 < 0.25), yet offered curious data shapes, similar to the piecewise regression encountered with the leaf water potential. Although much data obtained in our study could not be used statistically in the same way, we believe the possibility itself warrants further exploration. For example, similar correlation and regression approaches have been applied to measurements of maximum daily trunk shrinkage on stem water potential and xylem sap flow in the pursuit of identifying apple irrigation thresholds (De Swaef et al. 2009). If consistent linkages between cost-effective scalable metrics and plant physiological function can be identified, they stand to improve developing decision support platforms.

Conclusion

A new, autonomous sensor-based irrigation platform was used to impose four levels of drought stress in greenhouse containerized 'Budagovsky 9' rootstocks grafted with three apple cultivars in effort to identify valuable associations between the soil matric potential and plant physiological indicators of drought stress. All scion cultivars encountered substantive desiccation and defoliation at –60 and –80 kPa beginning 7 to 10 d after the imposition of deficit. We recommend using media-specific

soil-water relationships in future research endeavors using autonomous sensor-based irrigation platforms to avoid premature decline of tree function. Analysis of variance suggested scion cultivar and deficit extremity significantly influence A and E rates, g_s, and NPQ_t significantly. Pearson's correlation matrices indicated all physiological parameters had an r vale \leq |0.43|. Nevertheless, supplemental nonlinear regression suggested potentially useful data shapes that, if refined, may prove valuable for irrigation decision support systems. The soil matric potential considered with predawn leaf water potential converged on a piecewise regression identifying a critical point of -30.6 kPa, below which the slope of leaf water potential is increased when subjected to additional decreases in the soil matric potential. Therefore, additional efforts to describe the relationship between arduous measurements of physiological function with scalable and autonomous monitoring technologies appears beneficial and is advised.

References Cited

- Bates D, Mächler M, Bolker B, Walker S. 2015. Fitting linear mixed-effect models using lme4. J Stat Softw. 67(1):1–48. https://doi.org/10. 18637/jss.v067.i01.
- Bhusal N, Han S-G, Yoon T-M. 2019. Impact of drought stress on photosynthetic response, leaf water potential, and stem sap flow in two cultivars of bi-leader apple trees (*Malus* × *domestica* Borkh.). Sci Hortic. 246:535–543. https://doi.org/10.1016/j.scienta.2018.11.021.
- Bhusal N, Park IH, Jeong S, Choi B-H, Han S-G, Yoon T-M. 2023. Photosynthetic traits and plant hydraulic dynamics in Gamhong apple cultivar under drought, waterlogging, and stress recovery periods. Sci Hortic. 321:112276. https://doi.org/10.1016/j.scienta.2023.112276.
- Bierer AM. 2023. Development of an open-source soil water potential management system for horticultural applications, "Open_Irr." HardwareX. 15:e00458. https://doi.org/10.1016/j.ohx.2023. e00458.
- Chaves MM, Pereira JS, Maroco J, Rodrigues ML, Ricardo CP, Osorio ML, Carvalho I Faria T, Pinheiro C. 2002. How plants cope with water stress in the field: Photosynthesis and growth. Ann Bot. 89(7):907–916. https://doi.org/10.1093/aob/mcf105.
- Davies FS, Lakso AN. 1979. Diurnal and seasonal changes in leaf water potential components and elastic properties in response to water stress in apple trees. Physiol Plant. 46(2):109–114. https:// doi.org/10.1111/j.1399-3054.1979.tb06541.x.
- De Swaef T, Steppe K, Lemeur R. 2009. Determining reference values for stem water potential and maximum daily trunk shrinkage in young apple trees based on plant responses to water deficit. Agric Water Manag. 96(4):541–550. https://doi.org/10.1016/j.agwat.2008.09.013.
- Genty B, Briantais J, Baker N. 1989. The relationship between the quantum yield of photosynthetic electron transport and quenching of chlorophyll fluorescence. Biochim Biophys Acta. 990:87–92. https://doi.org/10.1016/S0304-4165(89)80016-9.
- Granier C, Aguirrezabal L, Chenu K, Cookson SJ, Dauzat M, Hamard P, Thioux JJ, Rolland G, Bouchier-Combaud S, Lebaudy A, Muller B, Simonneau T, Tardieu F. 2006. PHENOPSIS, an automated platform for reproducible phenotyping

- of plant responses to soil water deficit in *Arabidopsis thaliana* permitted the identification of an accession with low sensitivity to soil water deficit. New Phytol. 169(3):623–635. https://doi.org/10.1111/j.1469-8137.2005.01609.x.
- Harrell F, Charles D. 2021. Hmisc: Harrell miscellaneous. In (Version 4.6-0) https://CRAN. R-project.org/package=Hmisc.
- Jiang X, He L. 2021. Investigation of effective irrigation strategies for high-density apple orchards in Pennsylvania. Agronomy. 11(4): 11040732. https:// doi.org/10.3390/agronomy11040732.
- Kanazawa A, Kramer D. 2002. In vivo modulation of nonphotochemical exciton quenching (NPQ) by regulation of the chloroplast ATP synthase. Proc Natl Acad Sci USA. 99(20):12789–12794. https://doi.org/10.1073/pnas.182427499.
- Kanazawa A, Ostendorf E, Kohzuma K, Hoh D, Strand DD, Sato-Cruz M, Savage L, Cruz JA, Fisher N, Froehlich JE, Kramer DM. 2017. Chloroplast ATP synthase modulation of the thylakoid proton motive force: Implications for photosystem I and photosystem II photoprotection. Front Plant Sci. 8:719. https://doi.org/ 10.3389/fpls.2017.00719.
- Kitajima M, Butle, W. 1975. Quenching of chlorophyll fluorescence and primary photochemistry in chloroplasts by dibromothymoquinone. Biochim Biophys Acta. 376:105–115. https://doi. org/10.1016/0005-2728(75)90209-1.
- Kuznetsova A, Brockhoff PB, Rune HB. 2017.

 Package: Tests in linear mixed effects models.

 J Stat Softw. 82(13):1–26. https://doi.org/10.
 18637/jss.v082.i13.
- Lakso A, Seeley E. 1978. Environmentally induced responses of apple tree photosynthesis. HortScience. 13(6):646–650. https://doi.org/10.21273/HORTSCI.13.6.646.
- Leong E, Rahardjo H. 1997. Review of soil-water characteristic curve equations. J Geotech Geoenviron Eng. December:1106–1117. https://doi.org/ 10.1061/(ASCE)1090-0241(1997)123:12(1106).
- Maotani T, Machida Y. 1980. Leaf water potential as an indicator of irrigation timing for satsuma mandarin trees in summer. J Jpn Soc Hortic Sci. 49(1):41–48. https://doi.org/10.2503/jjshs.49.41.
- McCauely DM, Nackley LL. 2022. Development of mini-lysimeter system for use in irrigation automation of container-grown crops. HardwareX. 11:e00298. https://doi.org/10.1016/j.ohx. 2022.e00298.
- Osroosh Y, Peters RT, Campbell CS, Zhang Q. 2016. Comparison of irrigation automation algorithms for drip-irrigated apple trees. Comput Electron Agric. 128:87–99. https://doi.org/10.1016/j.compag.2016.08.013.
- Osroosh Y, Troy Peters R, Campbell CS, Zhang Q. 2015. Automatic irrigation scheduling of apple trees using theoretical crop water stress index with an innovative dynamic threshold. Comput Electron Agric. 118:193–203. https://doi.org/10.1016/j.compag.2015.09.006.
- PP Systems. 2013. CIRAS-3 portable photosynthesis system: Operation manual. PP Systems, Amesbury, MA, USA.
- Raymond Hunt E, Daughtry CST. 2014. Chlorophyll meter calibrations for chlorophyll content using measured and simulated leaf transmittances. Agron J. 106(3):931–939. https://doi.org/10.2134/agronj13.0322.
- Reid M, Kalcsits L. 2020. Water deficit timing affects physiological drought response, fruit size, and bitter pit development for 'Honeycrisp' apple. Plants. 9(7):874. https://doi.org/10.3390/plants9070874.

- Rodriguez-Dominguez CM, Forner A, Martorell S, Choat B, Lopez R, Peters JMR, Pfautsch S, Mayr S, Carins-Murphy MR, McAdam SAM, Richardson F, Diaz-Espejo A, Hernandez-Santana V, Menezes-Silva PE, Torres-Ruiz JM, Batz TA, Sack L. 2022. Leaf water potential measurements using the pressure chamber: Synthetic testing of assumptions towards best practices for precision and accuracy. Plant Cell Environ. 45(7):2037–2061. https://doi.org/10.1111/pce.14330.
- Soil Survey Staff. 2021. Web soil survey. http://websoilsurvey.sc.egov.usda.gov/. [accessed 1 May 2022].
- Sooriyapathirana S, Ranaweera LT, Jayarathne HSM, Gayathree THI, Rathnayake P, Karunarathne SI, Thilakarathne S, Salih R, Weebadde CK, Weebadde CP. 2021. Photosynthetic phenomics of field- and greenhouse-grown amaranths vs. sensory and species delimits. Plant Phenomics. 2021:2539380. https://doi.org/10.34133/2021/2539380.
- Spinu V, Grolemund G, Wickham H, Vaughan D, Lyttle I, Costigan I, Law J, Mitarotonda D, Larmarange J, Boiser J, Lee C. 2023. lubridate: Make dealing with dates a little easier. Version 1.9.2. https://github.com/tidvverse/lubridate.
- Tang L, Lovatt CJ. 2022. Effects of water-deficit stress and gibberellic acid on floral gene expression and floral determinacy in 'Washington' navel orange. J Am Soc Hortic Sci. 147(4):183–195. https://doi.org/10.21273/jashs05213-22.
- Tietz S, Hall CC, Cruz JA, Kramer DM. 2017. NPQ(T): A chlorophyll fluorescence parameter for rapid estimation and imaging of non-photochemical quenching of excitons in photosystem-II-associated antenna complexes. Plant Cell Environ. 40(8):1243–1255. https://doi.org/10. 1111/pce.12924.
- Tworkoski T, Fazio G, Glenn M. 2016. Apple rootstock resistance to drought. Sci Hortic. 204:70–78. https://doi.org/10.1016/j.scienta.2016.01.047.
- University of Minnesota Extension. 2019. Soil moisture sensors for irrigation scheduling. https://extension.umn.edu/irrigation/soil-moisture-sensors-irrigation-scheduling#pros%2C-consand-costs-of-soil-water-tension-sensors-1751861. [accessed 1 May 2021].
- Wang Z, Li G, Sun H, Ma L, Guo Y, Zhao Z, Gao H, Mei L. 2018. Effects of drought stress on photosynthesis and photosynthetic electron transport chain in young apple tree leaves. Biol Open. 7(11):bio035279. https://doi.org/10.1242/bio.035279
- Wei T, Simko V, Levy M, Xie Y, Jin Y, Zemla J, Freidank M, Cai J, Protivinsky T. 2021. corrplot: Visualization of a correlation matrix. Version 0.92. https://github.com/taiyun/corrplot.
- Wickham H, Averick M, Bryan J, Chang W, McGowan LDA, François R, Grolemund G, Hayes A, Henry L, Hester J, Kuhn M, Pedersen TL, Miller E, Bache SM, Müller K, Ooms J, Robinson D, Seidel DP, Spinu V, Takahashi K, Vaughan D, Wilke C, Woo K, Yutani H. 2019. Welcome to the tidyverse. J Open Source Softw. 4(43):1686. https://doi.org/ 10.21105/joss.01686.
- Zivcak M, Kalaji H, Shao H, Olsovska K, Brestic M. 2014. Photosynthetic proton and electron transport in wheat leaves under prolonged moderate drought stress. J Photochem Photobiol. 137:107–115. https://doi.org/10.1016/j.jphotobiol. 2014.01.007.